Pharmacogn. Mag.
A multifaceted peer reviewed journal in the field of Pharmacognosy and Natural Products
www.phcog.com | www.phcog.net

ORIGINAL ARTICLE

A Combination of Vinorelbine and Oxaliplatin to Restrain the Progression of Non-Small Cell Lung Cancer via Inhibition of the PI3K/AKT/ABCG2 Axis

Xiang Wang, Qingqing Ding[1], Tongshan Wang[1], Weiping Xie, Mao Huang

Department of Respiratory and Critical Care Medicine, The First Affiliated Hospital of Nanjing Medical University, [1]Department of Oncology, The First Affiliated Hospital of Nanjing Medical University, China

Submitted: 23-Sep-2021 Revised: 27-Apr-2022 Accepted: 30-Apr-2022 Published: 23-Nov-2022

ABSTRACT

Background: This research explored the effects of vinorelbine combined with oxaliplatin on non-small cell lung cancer (NSCLC). **Materials and Methods:** NSCLC cells were treated with vinorelbine, oxaliplatin, and insulin-like growth factor-1 (IGF-1; phosphatidylinositol 3-kinase/protein kinase B (PI3K/AKT) pathway activator), and transfected with ATP-binding cassette subfamily G member 2 (ABCG2) overexpression plasmid and silenced ABCG2 (siABCG2). Cell viability was detected by cell counting kit-8 assay, cell migration and invasion by the transwell assay, and cell apoptosis by flow cytometry. Levels of ABCG2, PI3K, phosphorylation (p)-PI3K, AKT, and p-AKT were evaluated through qRT-PCR and western blot. **Results:** Co-treatment with vinorelbine and oxaliplatin exerted synergistic effects in suppressing the proliferation, migration, invasion, and the phosphorylation of PI3K and AKT, and inhibiting ABCG2 expression while inducing apoptosis in NSCLC cells. Overexpression of ABCG2 reversed these effects on proliferation, migration, invasion, and apoptosis, while not affecting the PI3K/AKT pathway in NSCLC cells. IGF-1 inhibited the synergistic effect of vinorelbine and oxaliplatin on the NSCLC cells. Moreover, siABCG2 reversed the effects of IGF-1 on ABCG2 expression, and other cellular functions mentioned above in NSCLC cells receiving the co-treatment. **Conclusion:** A combination of vinorelbine with oxaliplatin represses the proliferation, migration, and invasion of NSCLC cells, and facilitates apoptosis via inhibition of the PI3K/AKT/ABCG2 axis.

Key words: ABCG2, non-small cell lung cancer, oxaliplatin, PI3K/AKT, vinorelbine

SUMMARY

- Combination of Vinorelbine with oxaliplatin achieved synergistic effects on suppressing cell proliferation, migration, and invasion while inducing apoptosis in NSCLC.
- Synergism of vinorelbine and oxaliplatin was achieved via PI3K/AKT/ABCG2 axis.
- PI3K/AKT/ABCG2 axis might serve as a target for NSCLC treatment.

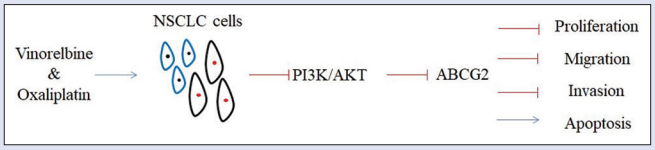

Abbreviations used: NSCLC = non-small cell lung cancer; siABCG2 = silencing ABCG2; CCK = cell counting kit; SCLC = small cell lung cancer; OD = optical density; qRT-PCR = Quantitative reverse transcription-polymerase chain reaction; ABC = ATP-binding cassette; ABCG2 = ABC subfamily G member 2.

Correspondence:

Dr. Xiang Wang,
Department of Respiratory and Critical Care Medicine, The First Affiliated Hospital of Nanjing Medical University, 300 Guangzhou Road, Gulou District, Nanjing, Jiangsu Province - 210 029, China.
E-mail: wangxiang_xwa@163.com

DOI: 10.4103/pm.pm_439_21

Access this article online
Website: www.phcog.com
Quick Response Code:

INTRODUCTION

In the wake of rising morbidity and mortality, cancer has become a major public health concern in China with the recent global cancer statistics stating that approximately 4,587,129 new cancer cases and 3,015,537 cancer deaths were reported in China in 2020.[1,2] Furthermore, lung cancer accounted for a considerable proportion of the cancer case-load, that is, 817,460 new lung cancer cases, in 2020 in China, making it one of the most common cancers. As the most frequently diagnosed malignant tumor and the foremost cause of cancer-associated fatality, lung cancer is generally classified into two primary histological types, non-small cell lung cancer (NSCLC) accounting for the majority (80–85%), and small cell lung cancer (SCLC).[3-5] As compared to SCLC, NSCLC is characterized by a slower rate of cell division and growth, as well as relatively late on-set of metastasis, and the diagnoses in the majority of patients are usually made at an advanced stage.[3,5-8] Multiple factors, such as smoking, air pollution, ionizing radiation genetics, and viral infection, are believed to increase the risk of NSCLC.[9-12] Traditionally, chemotherapy, radiotherapy, and surgery are the standard treatment approaches for NSCLC, among which chemotherapy is the first-line treatment for NSCLC and an inevitable choice for most patients.[13-15]

Vinorelbine, a fourth-generation semi-synthetic vinca alkaloid, is a well-tolerated chemotherapeutic drug used to treat various malignancies including NSCLC (having an effective rate of about 30%).[16-18] By binding to tubulin, vinorelbine can block the formation of the mitotic spindle and arrest the cell cycle at the G2/M phase, which eventually results in mitotic cell apoptosis.[19,20] Owing to its high selectivity for mitotic, instead of axonal microtubules,

Cite this article as: Wang X, Ding Q, Wang T, Xie W, Huang M. A combination of vinorelbine and oxaliplatin to restrain the progression of non-small cell lung cancer via inhibition of the PI3K/AKT/ABCG2 axis. Phcog Mag 2022;18:859-70.

vinorelbine preferentially targets cells undergoing division or with high proliferative ability,[17,21,22] and lesser damage to normal cells when used against tumor cells. Moreover, due to a broader anticancer spectrum and requirement of a lower therapeutic dose than other natural vinca alkaloids such as vincristine, vinorelbine has lower overall drug toxicity.[23,24]

As a third-generation platinum antitumor agent, following cisplatin and carboplatin, oxaliplatin is a diaminocycloexane-platinum complex demonstrating notable activity against different cancers including NSCLC.[25-27] Like other platinum agents, oxaliplatin facilitates the formation of a DNA adduct and inhibits DNA replication/transcription, finally bringing about apoptosis.[28] With no or incomplete cross-resistance against other platinum compounds, oxaliplatin has proven to be more effective than cisplatin, which can achieve equivalent cytotoxicity with fewer DNA adducts.[29,30] Moreover, oxaliplatin is considered relatively safe and manageable as it does not lead to nephrotoxicity, or gastrointestinal and hematological toxicity, resulting in lesser vomiting and nephropathy than cisplatin, and less myelosuppression than carboplatin.[26,28,31] Currently, a combination of vinorelbine with oxaliplatin is being studied in the clinical treatment of NSCLC[32]; however, the specific mechanisms underlying their action have not been elucidated.

Therefore, this research investigated the effects of vinorelbine combined with oxaliplatin on NSCLC and further probed into the underlying molecular mechanisms to offer novel insights into NSCLC treatment.

MATERIALS AND METHODS

Cell culture

Human NSCLC cell lines, H1299 and A549, were procured from American Type Culture Collection (ATCC; CRL-5803, CCL-185, Manassas, VA, USA). The H1299 cells were cultured in the RPMI-1640 medium (30-2001, ATCC, USA), whereas the Kaighn's Modified Ham's F-12 (F-12K) medium (30-2004, ATCC, USA) was utilized for incubation of A549 cells; fetal bovine serum (FBS; 30-2020, ATCC, USA) was added to all media in a final concentration of 10%. All cells were cultured in a humidified atmosphere maintained at 37°C containing 5% CO_2.

Cell treatment

Cells were divided into the following groups: control group (normal culture), NVB group, OXA group and CDG group. The vinorelbine (NVB) group cells were treated with 300 nM vinorelbine (KW-2307, Selleck Chemicals, Houston, TX, USA),[20] cells in the OXA group were treated with 10 μg/mL oxaliplatin (NSC 266046; Selleck Chemicals, USA),[33] and those in the CDG group were co-treated with 300 nM vinorelbine and 10 μg/mL oxaliplatin. Insulin-like growth factor-1 (IGF-1; NIST2926, Sigma-Aldrich, St. Louis, MO, USA) in a dose of 100 ng/mL served as an activator of the PI3K/AKT pathway.[34]

Cell transfection

In this research, the ABCG2-overexpression plasmid was constructed based on the pcDNA3.1/+vector (V79020, Thermo Fisher Scientific, USA), with the empty vector taken as the negative control (NC). The silenced ABCG2 (siABCG2; siG09827124503-1-5), and its negative control (siNC; siN0000001-1-10) were harvested from RiboBioBiotechnology Co., LTD (Guangzhou, China). The aforementioned plasmids or vectors were transfected into the A549 and NCI-H1299 cells using Lipo8000 (C0533, Beyotime Biotechnology, Shanghai, China). After cells were digested with trypsin solution (C0205, Beyotime Biotechnology, China), cells were seeded at a density of 4×10^5 cells/well in six well-plates and incubated until 80% confluence. Subsequently, 2.5 μg of plasmids or vectors, or 100 pmol small interfering RNAs (siRNAs) were mixed with 125 μL of Dulbecco's Modified Eagle Medium (DMEM; PM150210, Procell Life Science and Technology, Wuhan, China), and then 4 μL of Lipofectamine 8000 was added. For siRNA transfection, the mixture was incubated at room temperature for 20 min; this step was not required for plasmid transfection. Lastly, the mixture (125μL/well) was added to the plates and cells, followed by a continuous culture at 37°C for 24 or 48 h.

Cell counting kit (CCK-8) assay

Cell viability was assessed by a CCK-8 kit (C0040, Beyotime Biotechnology, China). After digestion with trypsin, 2000 cells were seeded in each well of the 96 well-plates and cultured for 24 or 48 h, followed by the addition of the CCK-8 solution (10 μL/well). After incubation at 37°C for another 1 h, a Synergy LX Multi-Mode microplate reader (BioTek Instruments, Inc., Winooski, VT, USA) was used to determine the optical density (OD) value at a wavelength of 450 nm.

Transwell assay

After getting trypsinized, the cells were washed with phosphate-buffered saline (PBS; C0221A, Beyotime Biotechnology, China) and then inoculated at a density of 1×10^5 cells/well in the upper chamber of a 24-well transwell chamber (351184, Corning Incorporation, Corning, NY, USA) pre-coated either without (for migration) or with (for invasion) Matrigel (354234, Corning Incorporation, USA). The upper chamber was filled with the serum-free medium, whereas the lower chamber contained the medium with 10% FBS. After a 48-h culture at 37°C, the migrated or invaded cells were fixed using 4% paraformaldehyde (P1110, Solarbio Science and Technology, Beijing, China) at 4°C for 30 min and stained using 0.1% crystal violet (G1063, Solarbio Science and Technology, China) at room temperature for half an hour, followed by observation under a NIB900 microscope (magnification: 250x; Yongxin Optics, Ningbo, China, http://www.yxopt.com/en/index.php).

Flow cytometry assay

The Annexin V-FITC/PI apoptosis detection kit (CA1020, Solarbio Science and Technology, China) was used to detect cell apoptosis. The cells were trypsinized, collected, and rinsed by cold PBS, followed by resuspended in 1 × binding buffer and centrifuged at 300 × g for 10 min. After removing the supernatant, cells were suspended in a 1 mL of 1 × binding buffer and adjusted to a concentration of 1×10^6 cells/mL. Subsequently, the 100 μL of cell suspension was mixed with 5μL of Annexin V-FITC in the dark at room temperature for 10 min. Next, 5 μL of propidium iodide (PI) was added and the cells were cultured in the dark at room temperature for another 5 min. Finally, 500 μL of PBS was added and the results were analyzed through a Multiskan™ FC flow cytometer (Thermo Fisher Scientific, USA).

Quantitative reverse transcription-polymerase chain reaction (qRT-PCR)

The Total RNA of the cells was isolated using the TRIzol reagent (15596026, Thermo Fisher Scientific, USA), and reverse transcription was undertaken to synthesize cDNA by SuperScript™ IV First-Strand Synthesis System (18091050, Thermo Fisher Scientific, USA). Then, cDNA amplification was traced with TB Green Fast qPCR Mix (RR430S, Takara Biomedical Technology, Beijing, China) in a CFX96 Touch real-time PCR detection system (Bio-Rad, Hercules, CA, USA) under predenaturation at 95°C for 30 s, as

well as 40 cycles at 95°C for 5 s and 60°C for 10 s. The loading control was glyceraldehyde-3-phosphate dehydrogenase (GAPDH) and the $2^{-\Delta\Delta CT}$ relative quantification method was used for data analysis.[35] The primer sequences (RiboBio, China) were listed as follows: ABCG2: forward, 5'-CAGGTGGAGGCAAATCTTCGT-3', reverse, 5'-ACCCTGTTAATCCGTTCGTTTT-3'; GAPDH: forward, 5'-GGAGCGAGATCCCTCCAAAAT-3', reverse, 5'-GGCTGTTGTCATACTTCTCATGG -3'.

Western blot

Cells were added to the radioimmunoprecipitation assay (RIPA) lysis buffer (C500007, Sangon Biotech, Shanghai, China) under centrifugation at 12830 × g and 4°C for 5 min, and the supernatant was collected to extract total protein from cells. Next, the protein concentration was evaluated by bicinchoninic acid (BCA) assay (C503021, Sangon Biotech, China). Equal amounts of marker (5 μL; PR1910, Solarbio Science and Technology, China) and protein (45 μg) were separated by sodium dodecyl sulfate-polyacrylamide gel electrophoresis (SDS-PAGE) with an SDS-PAGE preparation kit (C631100, Sangon Biotech, China) before transferring the protein to membranes (88585, Thermo Fisher Scientific, USA) blocked in 5% bovine serum albumin (BSA; E661003, Sangon Biotech, China) at room temperature for 1 h or 5% non-fat milk at room temperature for 90 min (for p-Akt). Subsequently, the membranes were cultured with primary antibodies against ABCG2 (rabbit, 1:1000; ab207732, Abcam, Cambridge, MA, USA), PI3K (1:1000; CY5355, Abways, shanghai, China), p-PI3K (1:1000; CY6427, Abways, USA), Akt (1:500; ab8805, Abcam, USA), p-Akt (1:500; ab38449, Abcam, USA), and GAPDH (mouse, 1:1000; ab9484, Abcam, USA) at 4°C overnight. After rinsing with Tris-buffered saline containing Tween 20 (TBST; C520009, Sangon Biotech, China), the membranes were incubated with the corresponding secondary antibodies – goat anti-rabbit IgG (ab205718, 1:2000; Abcam, USA) and goat anti-mouse IgG (ab205719, 1:2000; Abcam, USA) at room temperature for 1 h. Eventually, protein expression was visualized through eZwest Lite Auto Western Blotting System (Genscript, Piscataway, NJ, USA) combined with ECL luminescence reagent (C510043, Sangon Biotech, China); the Image J software (version 1.48, National Institutes of Health, Bethesda, MD, USA) was used to analyze the data.

Statistical analysis

Data were presented as the means ± standard deviation, and analyzed by Graphpad 8.0 (GraphPad Software Inc., San Diego, CA, USA). Multiple groups were compared using a one-way analysis of variance (ANOVA) followed by Tukey's *post hoc* test. A statistically significant difference was accepted when the P value was < 0.05.

RESULTS

Synergistic effects of the combination of vinorelbine with oxaliplatin in suppressing NSCLC cell progression and PI3K/AKT/ABCG2 pathway activation

As shown in Figure 1, the OD value, migration rate, and invasion rate were appreciably reduced in both A549 and NCI-H1299 cells after treatment with vinorelbine or oxaliplatin alone compared to the control group ($P < 0.05$). Furthermore, these trends were more pronounced in cells receiving the vinorelbine and oxaliplatin co-treatment ($P < 0.05$). On the contrary, flow cytometry assay exhibited a notable elevation in the apoptosis rate in A549 and NCI-H1299 cells treated with vinorelbine or oxaliplatin alone when compared to the cells under normal culture; the apoptosis rate of cells receiving co-treatment was found to be higher than those treated with individual drugs [$P < 0.001$, Figure 2a-d]. Besides, the protein levels of ABCG2, p-PI3K, and p-AKT in A549 and NCI-H1299 cells declined in the NVB and OXA groups as compared to the control group; a similar tendency was exhibited by the CDG group cells when compared with the NVB or OXA groups [$P < 0.001$, Figure 2e-h]. To summarize, the protein levels of PI3K and AKT varied across the four groups, with p-PI3K/PI3K and p-AKT/AKT of both cell lines reduced in the NVB and OXA groups when compared to the control group; the decreasing levels were more obvious in the CDG group [$P < 0.05$, Figure 2i-l].

ABCG2-overexpression reversed the effects of vinorelbine plus oxaliplatin on the proliferation, migration, invasion, and apoptosis of NSCLC cells

To investigate whether ABCG2 contributed to the functions of the combination of vinorelbine and oxaliplatin, the ABCG2-overexpression plasmid was transfected into the A549 and NCI-H1299 cells co-treated with vinorelbine and oxaliplatin, after which the transfection efficiency was tested by qRT-PCR. The results demonstrated that the ABCG2 mRNA level of the two cells receiving the co-treatment was lower than that of the cells under normal conditions. Additionally, cells receiving the vinorelbine-oxaliplatin co-treatment, along with transfection with ABCG2-overexpression plasmid, had a significantly elevated ABCG2 mRNA level in comparison with cells receiving the co-treatment and transfection with empty plasmid [$P < 0.001$, Figure 3a and b], indicating a successful transfection.

The OD value, migration rate, and invasion rate of both A549 and NCI-H1299 cells were declined in the CDG group when compared with the control group [$P < 0.001$, Figure 3c-l], whereas these indexes were raised in the CDG+ABCG2 group relative to the CDG+NC group [$P < 0.01$, Figure 3c-l]. Additionally, the apoptosis rate was increased in cells co-treated with vinorelbine and oxaliplatin, whereas the protein levels of ABCG2, p-PI3K, p-AKT, p-PI3K/PI3K, and p-AKT/AKT were reduced. Meanwhile, the ABCG2 protein expression of cells co-treated with vinorelbine and oxaliplatin and transfected with ABCG2-overexpression plasmid was higher than that of cells co-treated with vinorelbine and oxaliplatin and transfected with an empty plasmid. No statistically significant differences regarding the p-PI3K, p-AKT, p-PI3K/PI3K, and p-AKT/AKT levels were observed between the CDG+ABCG2 and CDG+NC groups[$P < 0.01$, Figure 4].

Combination of vinorelbine with oxaliplatin regulated the proliferation, migration, and apoptosis of NSCLC cells via the PI3K/AKT/ABCG2 axis

Using the western blot analysis, we observed that the A549 and NCI-H1299 cells in the CDG+IGF-1 group showed an upregulation of ABCG2, p-PI3K, p-AKT, p-PI3K/PI3K, and p-AKT/AKT relative to cells in the CDG group. Also, the protein level of ABCG2 was lowered in the CDG+IGF-1 + siABCG2 group when compared with the CDG+IGF-1 + siNC group. However, no obvious changes were observed in the levels of p-PI3K, p-AKT, p-PI3K/PI3K, and p-AKT/AKT between the CDG+IGF-1 + siABCG2 and CDG+IGF-1 + siNC groups [$P < 0.01$, Figure 5a-h].

The CCK-8 assay revealed that the OD value was notably elevated in A549 and NCI-H1299 cells co-treated with vinorelbine, oxaliplatin, and IGF-1 as compared to those treated with vinorelbine and oxaliplatin; the OD value of cells in the CDG+IGF-1 + siABCG2

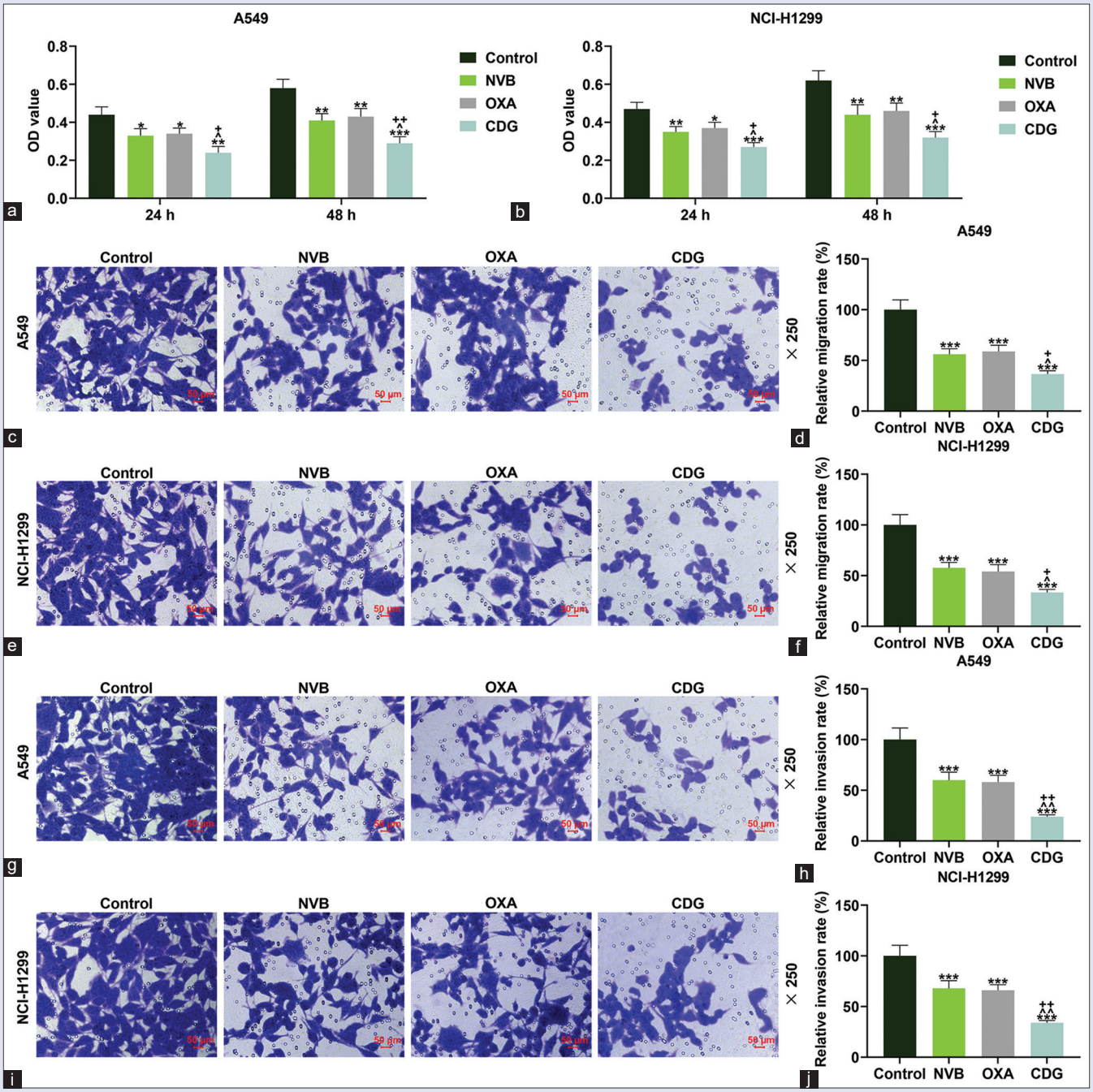

Figure 1: Combination of Vinorelbine with oxaliplatin achieved synergistic effects on suppressing the proliferation, migration, and invasion of NSCLC cells. (a and b) OD value at 24 or 48 h of A549 (a) and NCI-H1299 cells (b) was detected by CCK-8 assay after treatment of vinorelbine and oxaliplatin. (c) Representative images of A549 cell migration through Transwell assay after treatment of vinorelbine and oxaliplatin (scale: 50 μm; magnification: ×250). (d) The migration rate of A549 cells was tested by Transwell assay after treatment of vinorelbine and oxaliplatin. (e) Representative images of NCI-H1299 cell migration through Transwell assay after treatment of vinorelbine and oxaliplatin (scale: 50 μm; magnification: ×250). (f) The migration rate of NCI-H1299 cells was tested by Transwell assay after treatment of vinorelbine and oxaliplatin. (g) Representative images of A549 cell invasion through Transwell assay after treatment of vinorelbine and oxaliplatin (scale: 50 μm; magnification: ×250). (h) The invasion rate of A549 cells was tested by Transwell assay after treatment of vinorelbine and oxaliplatin. (i) Representative images of NCI-H1299 cell invasion through Transwell assay after treatment of vinorelbine and oxaliplatin (scale: 50 μm; magnification: ×250). (j) Invasion rate of NCI-H1299 cells was determined by Transwell assay after treatment of vinorelbine and oxaliplatin. * $P < 0.05$, ** $P < 0.01$, *** $P < 0.001$ vs. control group; ^$P < 0.05$, ^^$P < 0.01$ vs. NVB group; $^{+}P < 0.05$, $^{++}P < 0.01$ vs. OXA group. All experiments were repeated independently at least three times. Data were performed as the means ± standard deviation. NSCLC, non-small cell lung cancer; OD, optical density; CCK-8, cell counting kit-8; NVB, the group treated with vinorelbine; OXA, the group treated with oxaliplatin

group was lower than that of the CDG+IGF-1 + siNC group [$P < 0.05$, Figure 5i-j]. Similarly, the migration and invasion rates of A549 and NCI-H1299 cells in the CDG+IGF-1 group were higher than those of the CDG group; however, these two rates declined in the CDG+IGF-1 + siABCG2 group cells in contrast with the CDG+IGF-1 + siNC group [$P < 0.001$, Figure 6]. The opposite results

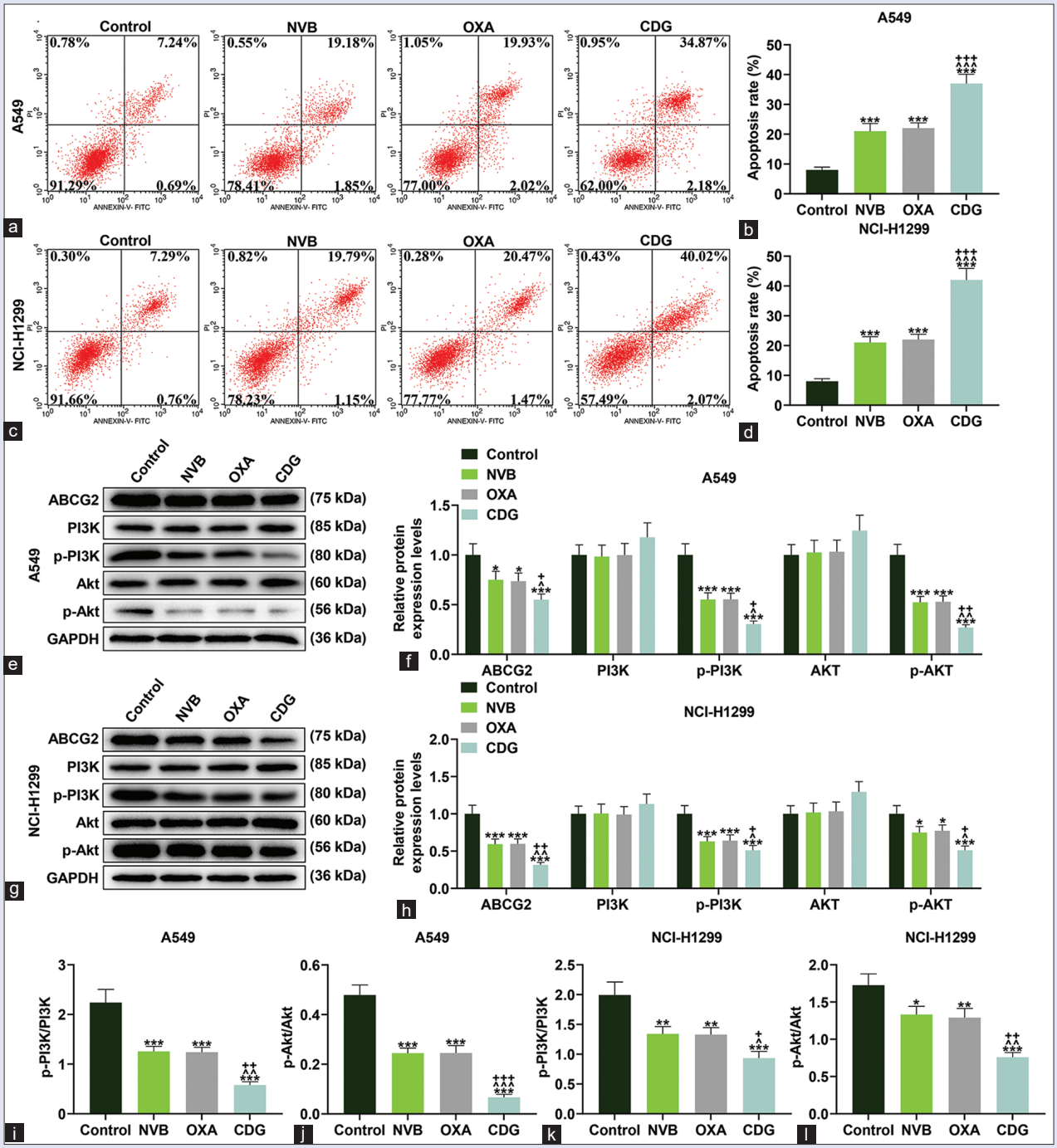

Figure 2: Combination of Vinorelbine with oxaliplatin achieved synergistic effects on inducing NSCLC cell apoptosis and inhibiting PI3K/AKT/ABCG2 pathway activation. (a) Representative images of A549 cell apoptosis through flow cytometry assay after treatment of vinorelbine and oxaliplatin. (b) The apoptosis rate of A549 cells was assessed by flow cytometry assay after treatment of vinorelbine and oxaliplatin. (c) Representative images of NCI-H1299 cell apoptosis through flow cytometry assay after treatment of vinorelbine and oxaliplatin. (d) The apoptosis rate of NCI-H1299 cells was assessed by flow cytometry assay after treatment of vinorelbine and oxaliplatin. (e) Protein bands of ABCG2, PI3K, p-PI3K, Akt, and p-Akt in A549 cells during western blot after treatment of vinorelbine and oxaliplatin. GAPDH was the loading control. (f) Protein levels of ABCG2, PI3K, p-PI3K, Akt, and p-Akt in A549 cells were evaluated through western blot after treatment of vinorelbine and oxaliplatin. GAPDH was the loading control. (g) Protein bands of ABCG2, PI3K, p-PI3K, Akt, and p-Akt in NCI-H1299 cells during western blot after treatment of vinorelbine and oxaliplatin. GAPDH was the loading control. (h) Protein levels of ABCG2, PI3K, p-PI3K, Akt, and p-Akt in NCI-H1299 cells were evaluated through western blot after treatment of vinorelbine and oxaliplatin. GAPDH was the loading control. (I and J) The levels of p-PI3K/PI3K (i) and p-Akt/Akt (j) in A549 cells were determined through western blot after treatment of vinorelbine and oxaliplatin. GAPDH was the loading control. (k and l) The levels of p-PI3K/PI3K (k) and p-Akt/Akt (l) in NCI-H1299 cells were measured through western blot after treatment of vinorelbine and oxaliplatin. GAPDH was the loading control. * $P < 0.05$, ** $P < 0.01$, *** $P < 0.001$ vs. control group; ^ $P < 0.05$, ^^ $P < 0.01$, ^^^ $P < 0.001$ vs. NVB group; $^{+}P < 0.05$, $^{++}P < 0.01$, $^{+++}P < 0.001$ vs. OXA group. All experiments were repeated independently at least three times. Data were presented as the means ± standard deviation. NSCLC, non-small cell lung cancer; p-, phosphorylation-; GAPDH, glyceraldehyde-3-phosphate dehydrogenase; NVB, the group treated with vinorelbine; OXA, the group treated with oxaliplatin

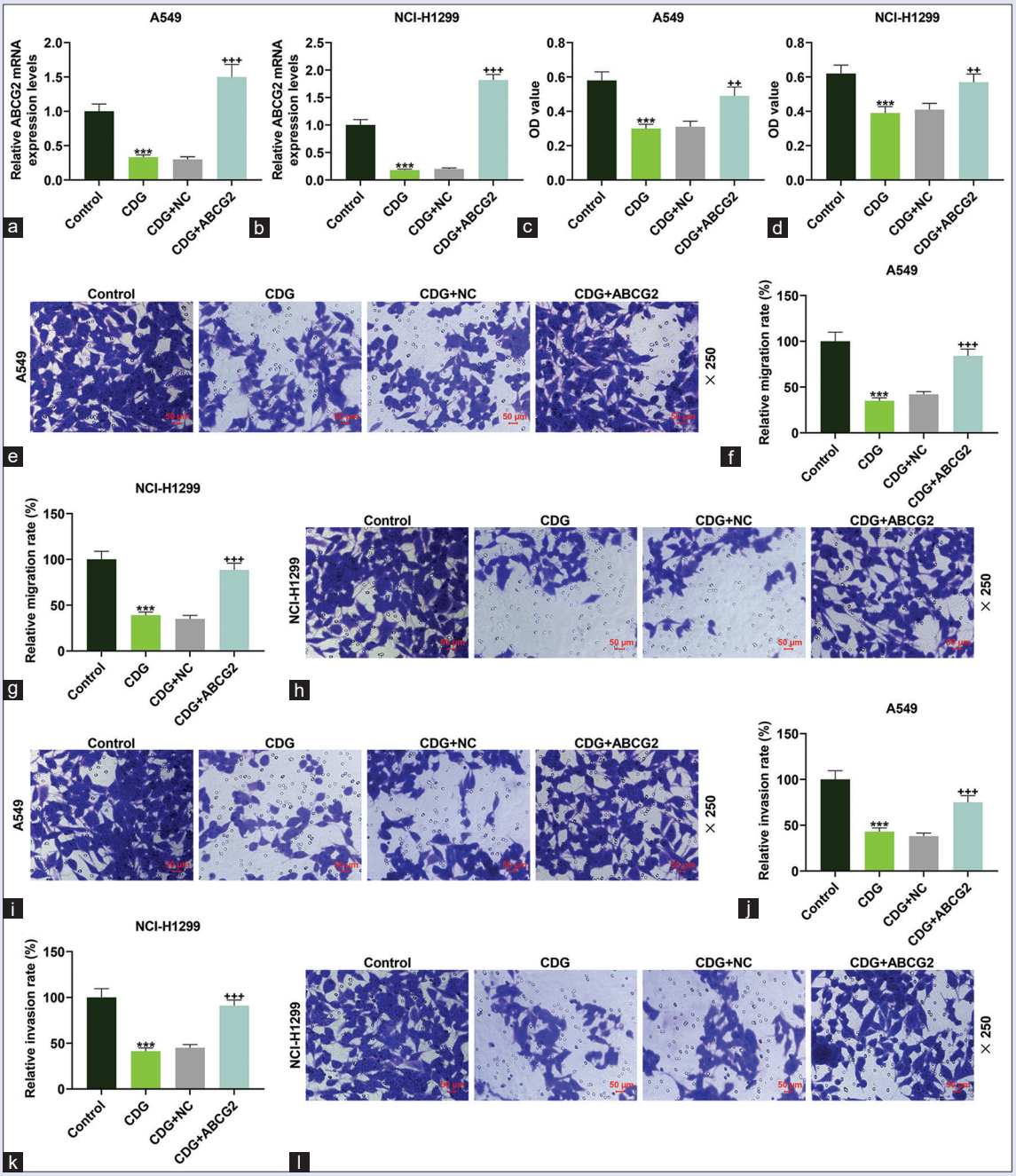

Figure 3: Overexpression ABCG2 reversed the effects of vinorelbine combined with oxaliplatin on the proliferation, migration, and invasion in NSCLC cells. (a and b) ABCG2 mRNA levels of A549 (a) and NCI-H1299 cells (b) were measured by qRT-PCR after treatment of vinorelbine and oxaliplatin and transfection of ABCG2 overexpression plasmid. GAPDH was the loading control. (c and d) OD value at 48 h of A549 (c) and NCI-H1299 cells (d) was detected by CCK-8 assay after treatment of vinorelbine and oxaliplatin and transfection of ABCG2 overexpression plasmid. (e) Representative images of A549 cell migration through Transwell assay after treatment of vinorelbine and oxaliplatin and transfection of ABCG2 overexpression plasmid (scale: 50 μm; magnification: ×250). (f) The migration rate of A549 cells was tested by Transwell assay after treatment of vinorelbine and oxaliplatin and transfection of ABCG2 overexpression plasmid. (g) The migration rate of NCI-H1299 cells was tested by Transwell assay after treatment of vinorelbine and oxaliplatin and transfection of ABCG2 overexpression plasmid. (h) Representative images of NCI-H1299 cell migration through Transwell assay after treatment of vinorelbine and oxaliplatin and transfection of ABCG2 overexpression plasmid (scale: 50 μm; magnification: ×250). (i) Representative images of A549 cell invasion through Transwell assay after treatment of vinorelbine and oxaliplatin and transfection of ABCG2 overexpression plasmid (scale: 50 μm; magnification: ×250). (j) Invasion rate of A549 cells was detected by Transwell assay after treatment of vinorelbine and oxaliplatin and transfection of ABCG2 overexpression plasmid. (k) Invasion rate of NCI-H1299 cells was examined by Transwell assay after treatment of vinorelbine and oxaliplatin and transfection of ABCG2 overexpression plasmid. (l) Representative images of NCI-H1299 cell invasion through Transwell assay after treatment of vinorelbine and oxaliplatin and transfection of ABCG2 overexpression plasmid (scale: 50 μm; magnification: ×250). *** $P < 0.001$ vs. control group; $^{++}P < 0.01$, $^{+++}P < 0.001$ vs. CDG+NC group. All experiments were repeated independently at least three times. Data were described as the means ± standard deviation. NSCLC, non-small cell lung cancer; qRT-PCR, quantitative reverse transcription-polymerase chain reaction; GAPDH, glyceraldehyde-3-phosphate dehydrogenase; OD, optical density; CCK-8, cell counting kit-8; CDG, the group co-treated with vinorelbine and oxaliplatin; NC, the negative control for ABCG2 overexpression plasmid

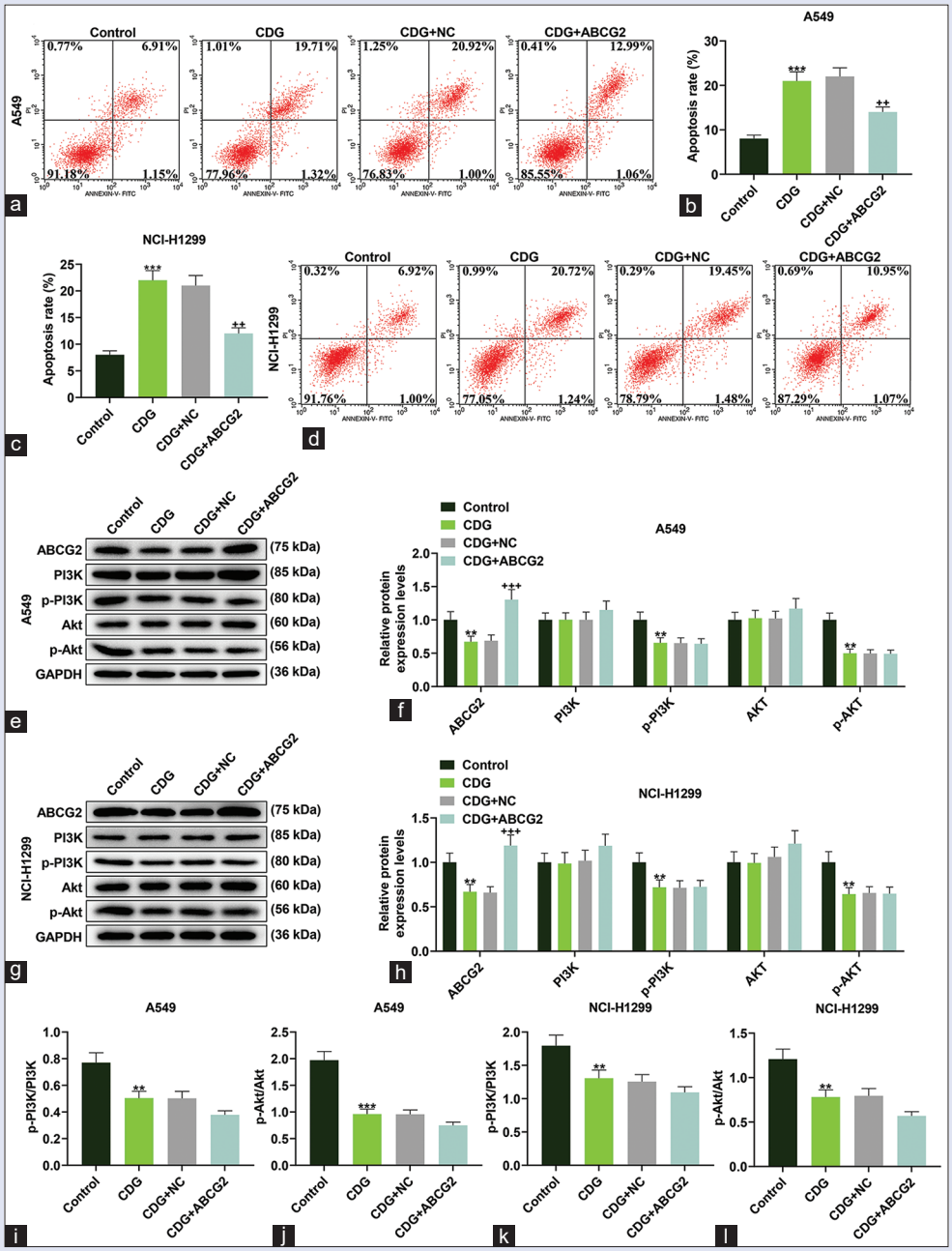

Figure 4: Overexpression ABCG2 reversed the effects of vinorelbine combined with oxaliplatin on NSCLC cell apoptosis and ABCG2 expression but did not affect PI3K/AKT pathway. (a) Representative images of A549 cell apoptosis through flow cytometry assay after treatment of vinorelbine and oxaliplatin and transfection of ABCG2 overexpression plasmid. (b) The apoptosis rate of A549 cells was assessed by flow cytometry assay after treatment of vinorelbine and oxaliplatin and transfection of ABCG2 overexpression plasmid. (c) The apoptosis rate of NCI-H1299 cells was evaluated by flow cytometry assay after treatment of vinorelbine and oxaliplatin and transfection of ABCG2 overexpression plasmid. (d) Representative images of NCI-H1299 cell apoptosis through flow cytometry assay after treatment of vinorelbine and oxaliplatin and transfection of ABCG2 overexpression plasmid. (e) Protein bands of ABCG2, PI3K, p-PI3K, Akt, and p-Akt in A549 cells during western blot after treatment of vinorelbine and oxaliplatin and transfection of ABCG2 overexpression plasmid. GAPDH was the loading control. (f) Protein levels of ABCG2, PI3K, p-PI3K, Akt, and p-Akt in A549 cells were evaluated through western blot after treatment of vinorelbine and oxaliplatin and transfection of ABCG2 overexpression plasmid. GAPDH was the loading control. (g) Protein bands of ABCG2, PI3K, p-PI3K, Akt, and p-Akt in NCI-H1299 cells during western blot after treatment of vinorelbine and oxaliplatin and transfection of ABCG2 overexpression plasmid. GAPDH was the loading control. (h) Protein levels of ABCG2, PI3K, p-PI3K, Akt, and p-Akt in NCI-H1299 cells were evaluated through western blot after treatment of vinorelbine and oxaliplatin and transfection of ABCG2 overexpression plasmid. GAPDH was the loading control. (i and j) The levels of p-PI3K/PI3K (i) and p-Akt/Akt (j) in A549 cells were determined through western blot after treatment of vinorelbine and oxaliplatin and transfection of ABCG2 overexpression plasmid. GAPDH was the loading control. (k and l) The levels of p-PI3K/PI3K (k) and p-Akt/Akt (l) in NCI-H1299 cells were detected through western blot after treatment of vinorelbine and oxaliplatin and transfection of ABCG2 overexpression plasmid. GAPDH was the loading control. ** $P < 0.01$, *** $P < 0.001$ vs. control group; $^{++}P < 0.01$, $^{+++}P < 0.001$ vs. CDG + NC group. All experiments were repeated independently at least three times. Data were exhibited as the means ± standard deviation. NSCLC, non-small cell lung cancer; p-, phosphorylation-; GAPDH, glyceraldehyde-3-phosphate dehydrogenase; CDG, the group co-treated with vinorelbine and oxaliplatin; NC, the negative control for ABCG2 overexpression plasmid

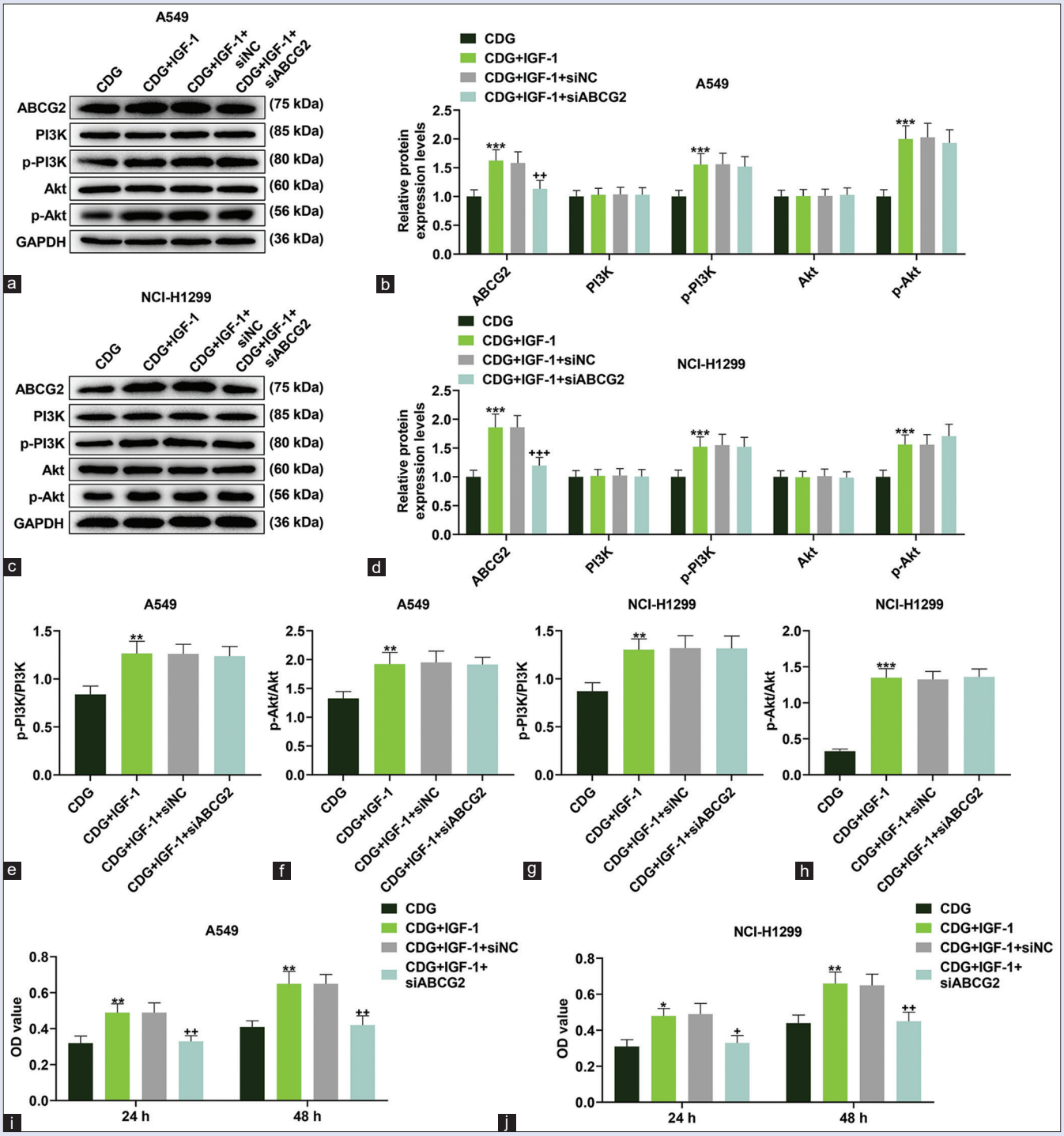

Figure 5: Combination of Vinorelbine with oxaliplatin suppressed NSCLC cell proliferation via PI3K/AKT/ABCG2 axis. (a) Protein bands of ABCG2, PI3K, p-PI3K, Akt, and p-Akt in A549 cells during western blot after treatment of vinorelbine, oxaliplatin, and IGF-1 and transfection of siABCG2. GAPDH was the loading control. (b) Protein levels of ABCG2, PI3K, p-PI3K, Akt, and p-Akt in A549 cells were evaluated through western blot after treatment of vinorelbine, oxaliplatin, and IGF-1 and transfection of siABCG2. GAPDH was the loading control. (c) Protein bands of ABCG2, PI3K, p-PI3K, Akt, and p-Akt in NCI-H1299 cells during western blot after treatment of vinorelbine, oxaliplatin, and IGF-1 and transfection of siABCG2. GAPDH was the loading control. (d) Protein levels of ABCG2, PI3K, p-PI3K, Akt, and p-Akt in NCI-H1299 cells were evaluated through western blot after treatment of vinorelbine, oxaliplatin, and IGF-1 and transfection of siABCG2. GAPDH was the loading control. (e and f) The levels of p-PI3K/PI3K (e) and p-Akt/Akt (f) in A549 cells were determined through western blot after treatment of vinorelbine, oxaliplatin, and IGF-1 and transfection of siABCG2. GAPDH was the loading control. (g and h) The levels of p-PI3K/PI3K (g) and p-Akt/Akt (h) in NCI-H1299 cells were measured through western blot after treatment of vinorelbine, oxaliplatin, and IGF-1 and transfection of siABCG2. GAPDH was the loading control. (i and j) OD value at 24 or 48 h of A549 (i) and NCI-H1299 cells (j) was detected by CCK-8 assay after treatment of vinorelbine, oxaliplatin, and IGF-1 and transfection of siABCG2. * $P < 0.05$, ** $P < 0.01$, *** $P < 0.001$ vs. CDG group; $^{+}P < 0.05$, $^{++}P < 0.01$ vs. CDG + IGF-1 + siNC group. All experiments were repeated independently at least three times. Data were displayed as the means ± standard deviation. NSCLC, non-small cell lung cancer; p-, phosphorylation-; siABCG2, silencing ABCG2; GAPDH, glyceraldehyde-3-phosphate dehydrogenase; OD, optical density; CCK-8, cell counting kit-8; CDG, the group co-treated with vinorelbine and oxaliplatin; siNC, the negative control for siABCG2

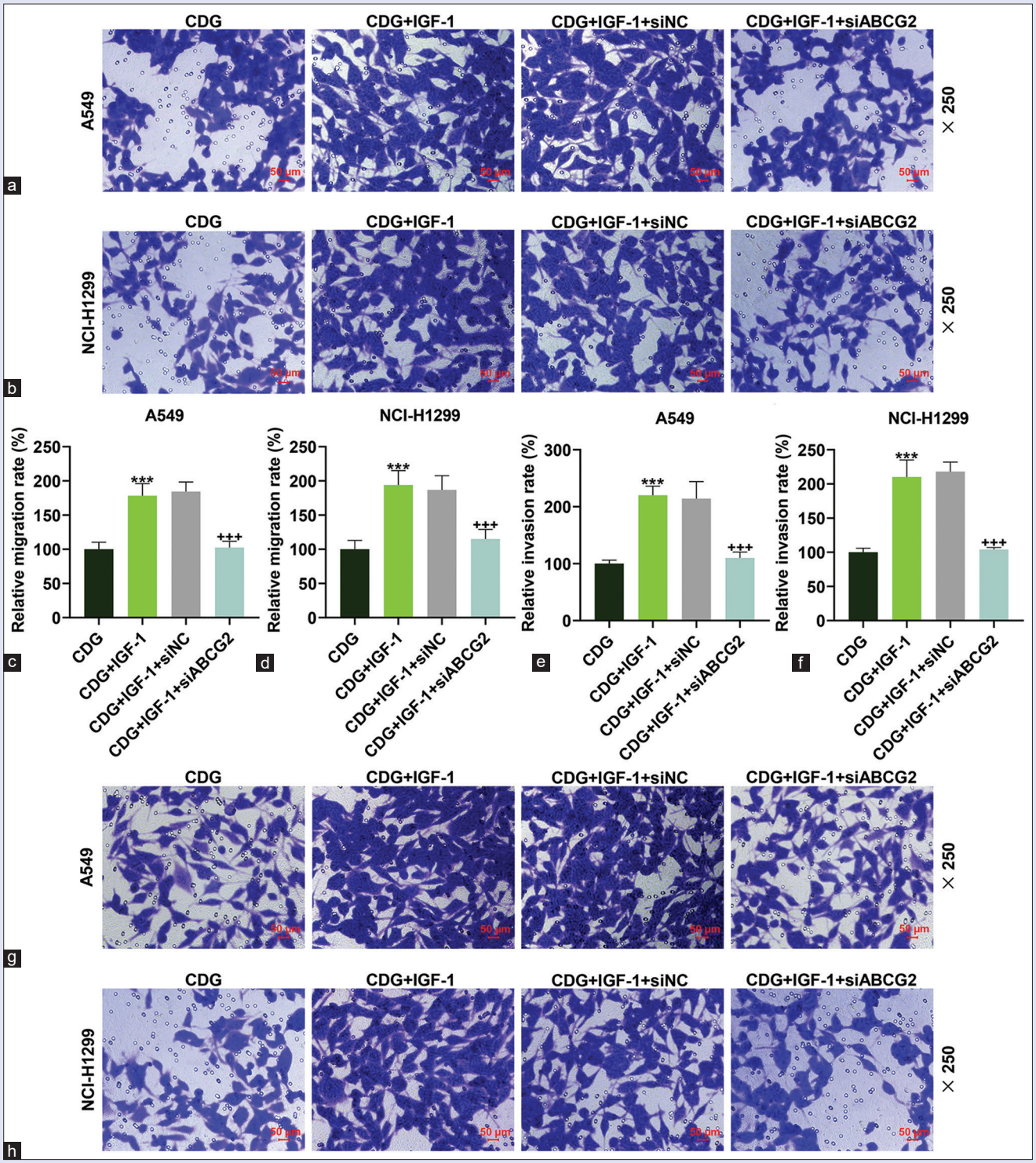

Figure 6: Combination of Vinorelbine with oxaliplatin repressed NSCLC cell migration and invasion via PI3K/AKT/ABCG2 axis. (a) Representative images of A549 cell migration through Transwell assay after treatment of vinorelbine, oxaliplatin, and IGF-1 and transfection of siABCG2 (scale: 50 μm; magnification: ×250). (b) Representative images of NCI-H1299 cell migration through Transwell assay after treatment of vinorelbine, oxaliplatin, and IGF-1 and transfection of siABCG2 (scale: 50 μm; magnification: ×250). (c) The migration rate of A549 cells was tested by Transwell assay after treatment of vinorelbine, oxaliplatin, and IGF-1 and transfection of siABCG2. (d) The migration rate of NCI-H1299 cells was tested by Transwell assay after treatment of vinorelbine, oxaliplatin, and IGF-1 and transfection of siABCG2. (e) The invasion rate of A549 cells was tested by Transwell assay after treatment of vinorelbine, oxaliplatin, and IGF-1 and transfection of siABCG2. (f) The invasion rate of NCI-H1299 cells was detected by Transwell assay after treatment of vinorelbine, oxaliplatin, and IGF-1 and transfection of siABCG2. (g) Representative images of A549 cell invasion through Transwell assay after treatment of vinorelbine, oxaliplatin, and IGF-1 and transfection of siABCG2 (scale: 50 μm; magnification: ×250). (h) Representative images of NCI-H1299 cell invasion through Transwell assay after treatment of vinorelbine, oxaliplatin, and IGF-1 and transfection of siABCG2 (scale: 50 μm; magnification: ×250). *** $P < 0.001$ vs. CDG group; $^{+++}P < 0.001$ vs. CDG+IGF-1 + siNC group. All experiments were repeated independently at least three times. Data were shown as the means ± standard deviation . NSCLC, non-small cell lung cancer; siABCG2, silencing ABCG2; CDG, the group co-treated with vinorelbine and oxaliplatin; siNC, the negative control for siABCG2

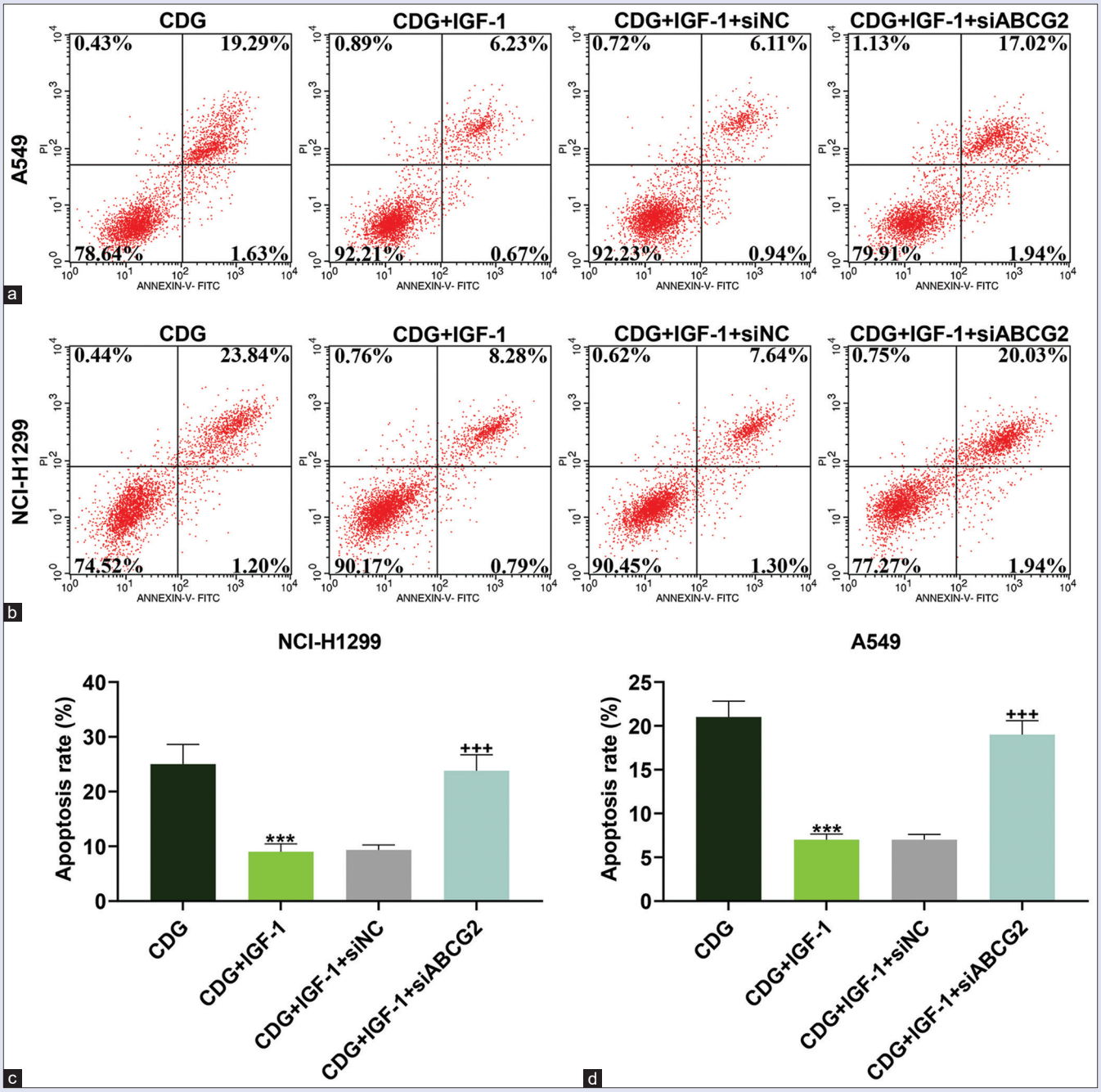

Figure 7: Combination of Vinorelbine with oxaliplatin promoted NSCLC cell apoptosis via PI3K/AKT/ABCG2 axis. (a) Representative images of A549 cell apoptosis through flow cytometry assay after treatment of vinorelbine, oxaliplatin, and IGF-1 and transfection of siABCG2. (b) Representative images of NCI-H1299 cell apoptosis through flow cytometry assay after treatment of vinorelbine, oxaliplatin, and IGF-1 and transfection of siABCG2. (c) The apoptosis rate of A549 cells was assessed by flow cytometry assay after treatment of vinorelbine, oxaliplatin, and IGF-1 and transfection of siABCG2. (d) The apoptosis rate of NCI-H1299 cells was evaluated by flow cytometry assay after treatment of vinorelbine, oxaliplatin, and IGF-1 and transfection of siABCG2. *** $P < 0.001$ vs. CDG group; $^{+++}P < 0.001$ vs. CDG+IGF-1+siNC group. All experiments were repeated independently at least three times. Data were expressed as the means ± standard deviation. NSCLC, non-small cell lung cancer; siABCG2, silencing ABCG2; CDG, the group co-treated with vinorelbine and oxaliplatin; siNC, the negative control for siABCG2

were obtained during the detection of cell apoptosis rate [$P < 0.001$, Figure 7].

DISCUSSION

Vinorelbine and oxaliplatin are common chemotherapeutic drugs utilized in several malignant tumors, including NSCLC.[18,26] Although the effectiveness of a combination of vinorelbine with oxaliplatin in the treatment of NSCLC has been validated by many researchers,[32,36-40] the underlying mechanisms of action remain unclear. We intended to explore the effects of this combination on NSCLC by treating NSCLC cells with vinorelbine and oxaliplatin *in vitro*. Similar to a previous study about the combination of lenvatinib and vinorelbine in anaplastic

thyroid cancer,[41] we observed that both drugs could repress cell proliferation, migration, and invasion while promoting apoptosis, and a combination of the two further enhanced these effects, which highlights the synergistic activity of vinorelbine with oxaliplatin on NSCLC.

ATP-binding cassette (ABC) transporters, a group of molecules that modulate the energy (from ATP-hydrolysis)-dependent transport of multiple substrates across the cell membrane against a concentration gradient, are widely acknowledged as responsible for the most common mechanism underlying multidrug resistance.[42] As a member of that group, ABC subfamily-G member-2 (ABCG2) has been reported to be conducive to drug resistance via the outflow of intracellular drugs.[42-44] Additionally, a previous study demonstrated that ABCG2 is activated to mitigate apoptosis induced by endoplasmic reticulum (ER) stress in oxaliplatin-resistant colorectal cancer cells.[27] Furthermore, it is worth noting that the PI3K/AKT pathway mediates ABCG2 to participate in the chemotherapeutic resistance of human multiple myeloma and malignant pleural mesothelioma.[45,46] The PI3K/AKT signaling pathway plays a crucial role in cancer occurrence and advancement, in which the phosphorylation of activated PI3K brings about AKT activation, which in turn, affects the downstream targets to regulate diverse cellular processes, such as proliferation, metastasis, and survival.[45,47-49] Considering all these findings, it was logical to presume that a combination of vinorelbine and oxaliplatin may enhance the therapeutic effects by suppressing ABCG2 expression, which is probably realized via inhibition of the PI3K/AKT pathway. In our experiments, both vinorelbine and oxaliplatin inhibited activation of PI3K, AKT, and ABCG2, and the inhibition was augmented when the cells were co-treated with the two drugs. This implies that the PI3K/AKT/ABCG2 pathway may be associated with the synergism of vinorelbine and oxaliplatin against NSCLC.

Furthermore, we investigated specific mechanisms underlying the therapeutic effects of vinorelbine combined with oxaliplatin on NSCLC based on the aforementioned hypothesis. To address this, cells were co-treated with vinorelbine and oxaliplatin and transfected with ABCG2-overexpression plasmid for validating the participation of ABCG2. We observed that ABCG2 overexpression reversed the effects of vinorelbine plus oxaliplatin in suppressing cell proliferation, migration, and invasion, as well as promoting cell apoptosis in NSCLC, which confirmed our hypothesis that vinorelbine plus oxaliplatin exerted a synergistic by repressing ABCG2. Moreover, we found that the overexpressed ABCG2 did not affect the combination therapy-induced inhibition of the PI3K/AKT pathway, indicating that ABCG2 might be the downstream gene for this signaling pathway. Based on these findings, we further investigated the relationship between the PI3K/AKT pathway, ABCG2, and the combination therapy by constructing an ABCG2-silence model and treating the NSCLC cells co-treated with vinorelbine and oxaliplatin with the PI3K/AKT pathway activator, IGF-1. It was observed that the PI3K/AKT pathway can modulate the protein level of ABCG2 in NCI-H929 cells, and its inhibition reverses the protective effects of ABCG2 against chemotherapeutic agents in multiple myeloma.[45] Likewise, in our study, the results of western blot analysis showed that the activation of the PI3K/AKT pathway positively regulated ABCG2 levels in NSCLC cells, whereas the knockdown of ABCG2 did not affect the PI3K/AKT pathway, confirming the recognition of ABCG2 as the downstream target for the PI3K/AKT pathway. In this study, we found that the PI3K/AKT pathway regulated ABCG2 to mediate cell proliferation, migration, invasion, and apoptosis during the action of vinorelbine combined with oxaliplatin on NSCLC.

CONCLUSION

In summary, the present research successfully determined the synergistic effects of vinorelbine and oxaliplatin in suppressing NSCLC cell progression and further probed into the specific mechanism of action. It also demonstrated that the desired effects of the combination therapy were achieved via inhibition of the PI3K/AKT/ABCG2 axis. This research offers novel insights into the therapeutic effects of vinorelbine combined with oxaliplatin on NSCLC and provides a new approach for NSCLC treatment by targeting the PI3K/AKT/ABCG2 axis.

Conflicts of interest

There are no conflicts of interest.

Financial support and sponsorship

Nil.

REFERENCES

1. Sung H, Ferlay J, Siegel RL, Laversanne M, Soerjomataram I, Jemal A, *et al.* Global Cancer Statistics 2020: GLOBOCAN estimates of incidence and mortality worldwide for 36 cancers in 185 countries. CACancer JClin 2021;71:209-49.
2. Cao W, Chen HD, Yu YW, Li N, Chen WQ. Changing profiles of cancer burden worldwide and in China: Asecondary analysis of the global cancer statistics 2020. ChinMed J 2021;134:783-91.
3. Cai Y, Sheng Z, Liang S. Radiosensitization effects of curcumin plus cisplatin on non-small cell lung cancer A549 cells. OncolLett 2019;18:529-34.
4. Chen W, Zheng R, Baade PD, Zhang S, Zeng H, Bray F, *et al.* Cancer statistics in China, 2015. CACancer JClin 2016;66:115-32.
5. Zhang X, Li Y, Qi P, Ma Z. Biology of MiR-17-92 cluster and its progress in lung cancer. IntJMed Sci 2018;15:1443-8.
6. Li D, Meng D, Niu R. Exosome-reversed chemoresistance to cisplatin in non-small lung cancer through transferring miR-613. Cancer ManagRes 2020;12:7961-72.
7. Wang P, Liu X, Shao Y, Wang H, Liang C, Han B, *et al.* MicroRNA-107-5p suppresses non-small cell lung cancer by directly targeting oncogene epidermal growth factor receptor. Oncotarget 2017;8:57012-23.
8. Zhang XC, Wang J, Shao GG, Wang Q, Qu X, Wang B, *et al.* Comprehensive genomic and immunological characterization of Chinese non-small cell lung cancer patients. NatCommun 2019;10:1772.
9. Li G, Mei Y, Yang F, Yi S, Wang L. Identification of genome variations in patients with lung adenocarcinoma using whole genome re-sequencing. MolMed Rep 2017;16:9464-72.
10. Chang KH, Tsai SC, Lee CY, Chou RH, Fan HC, Lin FC, *et al.* Increased Risk of Sensorineural Hearing Loss as a Result of Exposure to Air Pollution. IntJEnviron ResPublic Health 2020;17:1969.
11. Thun MJ, Hannan LM, Adams-Campbell LL, Boffetta P, Buring JE, Feskanich D, *et al.* Lung cancer occurrence in never-smokers: An analysis of 13 cohorts and 22 cancer registry studies. PLoS Med 2008;5:e185.
12. Liu W, Tan X, Shu L, Sun H, Song J, Jin P, *et al.* Ursolic acid inhibits cigarette smoke extract-induced human bronchial epithelial cell injury and prevents development of lung cancer. Molecules (Basel, Switzerland) 2012;17:9104-15.
13. Yu S, Geng S, Hu Y. miR-486-5p inhibits cell proliferation and invasion through repressing GAB2 in non-small cell lung cancer. OncolLett 2018;16:3525-30.
14. Kiura K, Imamura F, Kagamu H, Matsumoto S, Hida T, Nakagawa K, *et al.* Phase 3 study of ceritinib vs chemotherapy in ALK-rearranged NSCLC patients previously treated with chemotherapy and crizotinib (ASCEND-5): Japanese subset. JpnJClin Oncol 2018;48:367-75.
15. Pan S, Wang F, Huang P, Xu T, Zhang L, Xu J, *et al.* The study on newly developed McAb NJ001 specific to non-small cell lung cancer and its biological characteristics. PLoS One 2012;7:e33009.
16. Altinoz MA, Ozpinar A, Alturfan EE, Elmaci I. Vinorelbine's anti-tumor actions may depend on the mitotic apoptosis, autophagy and inflammation: Hypotheses with implications for chemo-immunotherapy of advanced cancers and pediatric gliomas. JChemother (Florence, Italy) 2018;30:203-12.
17. Hastie R, Lim E, Sluka P, Campbell L, Horne AW, Ellett L, *et al.* Vinorelbine potently induces

placental cell death, does not harm fertility and is a potential treatment for ectopic pregnancy. EBioMedicine 2018;29:166-76.

18. Furuse K, Kubota K, Kawahara M, Ogawara M, Kinuwaki E, Motomiya M, *et al.* A phase II study of vinorelbine, a new derivative of vinca alkaloid, for previously untreated advanced non-small cell lung cancer. Japan Vinorelbine Lung Cancer Study Group. Lung cancer (Amsterdam, Netherlands) 1994;11:385-91.
19. Wang LG, Liu XM, Kreis W, Budman DR. The effect of antimicrotubule agents on signal transduction pathways of apoptosis: Areview. Cancer ChemotherPharmacol 1999;44:355-61.
20. Zhang M, Boyer M, Rivory L, Hong A, Clarke S, Stevens G, *et al.* Radiosensitization of vinorelbine and gemcitabine in NCI-H460 non-small-cell lung cancer cells. IntJRadiat OncolBiolPhys 2004;58:353-60.
21. Binet S, Fellous A, Lataste H, Krikorian A, Couzinier JP, Meininger V. *In situ* analysis of the action of Navelbine on various types of microtubules using immunofluorescence. SeminOncol 1989;16:5-8.
22. Paintrand MR, Pignot I. Navelbine: An ultrastructural study of its effects. JElectron Microsc 1983;32:115-24.
23. Levêque D, Jehl F. Clinical pharmacokinetics of vinorelbine. ClinPharmacokinet 1996;31:184-97.
24. Topletz AR, Dennison JB, Barbuch RJ, Hadden CE, Hall SD, Renbarger JL. The relative contributions of CYP3A4 and CYP3A5 to the metabolism of vinorelbine. Drug MetabDispos 2013;41:1651-61.
25. Esim O, Bakirhan NK, Yildirim N, Sarper M, Savaser A, Ozkan SA, *et al.* Development, optimization and *in vitro* evaluation of oxaliplatin loaded nanoparticles in non-small cell lung cancer. Daru 2020;28:673-84.
26. Monnet I, Brienza S, Hugret F, Voisin S, Gastiaburu J, Saltiel JC, *et al.* Phase II study of oxaliplatin in poor-prognosis non-small cell lung cancer (NSCLC). ATTIT. Association pour le Traitement des Tumeurs Intra Thoraciques. EurJCancer 1998;34:1124-7.
27. Hsu HH, Chen MC, Baskaran R, Lin YM, Day CH, Lin YJ, *et al.* Oxaliplatin resistance in colorectal cancer cells is mediated via activation of ABCG2 to alleviate ER stress induced apoptosis. JCell Physiol 2018;233:5458-67.
28. Raez LE, Santos ES, Lopes G, Rosado MF, Negret LM, Rocha-Lima C, *et al.* Efficacy and safety of oxaliplatin and docetaxel in patients with locally advanced and metastatic non-small-cell lung cancer (NSCLC). Lung Cancer (Amsterdam, Netherlands) 2006;53:347-53.
29. Cvitkovic E. Ongoing and unsaid on oxaliplatin: The hope. BrJCancer 1998;77(Suppl 4):8-11.
30. Mathé G, Kidani Y, Segiguchi M, Eriguchi M, Fredj G, Peytavin G, *et al.* Oxalato-platinum or 1-OHP, a third-generation platinum complex: An experimental and clinical appraisal and preliminary comparison with cis-platinum and carboplatinum. BiomedPharmacother 1989;43:237-50.
31. Kakolyris S, Ziras N, Vamvakas L, Varthalitis J, Papakotoulas P, Syrigos K, *et al.* Gemcitabine plus oxaliplatin combination (GEMOX regimen) in pretreated patients with advanced non-small cell lung cancer (NSCLC): Amulticenter phase II study. Lung Cancer (Amsterdam, Netherlands) 2006;54:347-52.
32. Monnet I, Soulié P, de Cremoux H, Saltiel-Voisin S, Bekradda M, Saltiel JC, *et al.* Phase I/II study of escalating doses of vinorelbine in combination with oxaliplatin in patients with advanced non-small-cell lung cancer. JClin Oncol 2001;19:458-63.
33. Segura E, Durand M, Amigorena S. Similar antigen cross-presentation capacity and phagocytic functions in all freshly isolated human lymphoid organ-resident dendritic cells. JExp Med 2013;210:1035-47.
34. Xu FF, Zhu H, Li XM, Yang F, Chen JD, Tang B, *et al.* Intercellular adhesion molecule-1 inhibits osteogenic differentiation of mesenchymal stem cells and impairs bio-scaffold-mediated bone regeneration in vivo. Tissue Eng Part A 2014;20:2768-82.
35. Livak KJ, Schmittgen TD. Analysis of relative gene expression data using real-time quantitative PCR and the 2(-Delta Delta C (T)) Method. Methods 2001;25:402-8.
36. Gao JF, Zhang XH, Wang J, Rao ZG, Zhu YZ, Ou WL, *et al.* [Efficacy of NO regimen and NP regimen on advanced non-small cell lung cancer: Aprospective randomized trial]. Ai Zheng 2005;24:990-3.
37. Yao W, Zhou H, Wei Y, Wang G, Wang Y. [Oxaliplatin combined with vinorelbine in the treatment of patients with advanced non-small cell lung cancer]. Zhongguo Fei Ai Za Zhi 2005;8:227-9.
38. Monnet I, de CH, Soulié P, Saltiel-Voisin S, Bekradda M, Saltiel JC, *et al.* Oxaliplatin plus vinorelbine in advanced non-small-cell lung cancer: Final results of a multicenter phase II study. AnnOncol 2002;13:103-7.
39. Mir O, Alexandre J, Ropert S, Montheil V, Martin I, Durand JP, *et al.* Vinorelbine and oxaliplatin in stage IV nonsmall cell lung cancer patients unfit for cisplatin: Asingle-center experience. Anticancer Drugs 2009;20:105-8.
40. Liu X, Ma L, Yang K, Tian J. [Vinorelbine plus oxaliplatin versus vinorelbine plus cisplatin for advanced non-small cell lung cancer: Asystematic review]. Zhongguo Fei Ai Za 2010;13:112-7.
41. Di Desidero T, Orlandi P, Gentile D, Banchi M, Alì G, Kusmic C, *et al.* Pharmacological effects of vinorelbine in combination with lenvatinib in anaplastic thyroid cancer. PharmacolRes2020;158:104920.
42. Robey RW, Polgar O, Deeken J, To KW, Bates SE. ABCG2: Determining its relevance in clinical drug resistance. Cancer Metastasis Rev 2007;26:39-57.
43. Chang FW, Fan HC, Liu JM, Fan TP, Jing J, Yang CL, *et al.* Estrogen enhances the expression of the multidrug transporter gene ABCG2-increasing drug resistance of breast cancer cells through estrogen receptors. IntJMol Sci 2017;18:163.
44. Stacy AE, Jansson PJ, Richardson DR. Molecular pharmacology of ABCG2 and its role in chemoresistance. MolPharmacol 2013;84:655-69.
45. Wang L, Lin N, Li Y. The PI3K/AKT signaling pathway regulates ABCG2 expression and confers resistance to chemotherapy in human multiple myeloma. OncolRep 2019;41:1678-90.
46. Fischer B, Frei C, Moura U, Stahel R, Felley-Bosco E. Inhibition of phosphoinositide-3 kinase pathway down regulates ABCG2 function and sensitizes malignant pleural mesothelioma to chemotherapy. Lung Cancer (Amsterdam, Netherlands) 2012;78:23-9.
47. Gou XJ, Bai HH, Liu LW, Chen HY, Shi Q, Chang LS, *et al.* Asiatic acid interferes with invasion and proliferation of breast cancer cells by inhibiting wave3 activation through PI3K/AKT signaling pathway. Biomed Res Int 2020;2020:1874387.
48. Xu J, Wang J, Zhang S. Mechanisms of resistance to irreversible epidermal growth factor receptor tyrosine kinase inhibitors and therapeutic strategies in non-small cell lung cancer. Oncotarget 2017;8:90557-78.
49. Dong J, Li J, Li J, Cui L, Meng X, Qu Y, *et al.* The proliferative effect of cortisol on bovine endometrial epithelial cells. ReprodBioEndocrinol 2019;17:97.